RSC Advances

ROYAL SOCIETY OF CHEMISTRY

www.rsc.org/advances

N,N-Diarylamino End-capping Towards a New Strategy for Simultaneously Enhancement Open-Circuit Voltage, Short-Circuit Current Density and Fill Factor in Small Molecule Organic Solar Cells †

Daobin Yang, ‡[a] Youqin Zhu, ‡[b] Yan Jiao, [a] Lin Yang, [a] Qianqian Yang, [b] Qian Luo, [a] Xuemei Pu, [a] Yan Huang, *[a] Suling Zhao, *[b] and Zhiyun Lu *[a]

[a] *Key Laboratory of Green Chemistry and Technology (Ministry of Education), College of Chemistry, Sichuan University, Chengdu 610064, P. R. China. E-mail: huangyan@scu.edu.cn; luzhiyun@scu.edu.cn*

[b] *Key Laboratory of Luminescence and Optical Information (Ministry of Education), Institute of Optoelectronics Technology, Beijing Jiaotong University, Beijing 100044, P. R. China. E-mail: slzhao@bjtu.edu.cn*

† Electronic supplementary information (ESI) available: CV curves and AFM images.

‡ The first two authors contributed equally to this work.

Abstract: A series of new asymmetrical squaraine derivatives bearing *N,N*-diarylamino substituents as end-capping groups, namely ASQAr-1~6, were designed and synthesized. In comparison with the reference compound ASQB bearing a *N,N*-diisobutylamino end-capper, all the six target compounds exhibit improved thermal stability, more red-shifted and broadened absorption band as well as lower HOMO and LUMO energy levels. Despite the hole mobility of most of the objective compounds is lower than that of ASQB, solution-processed bulk-heterojunction small molecule organic solar cells (BHJ-SMOSCs) using ASQAr-1~6 as electron donor materials all show drastically higher power conversion efficiency (PCE, 3.08~3.69%) than that of the ASQB-based reference device (PCE=1.54%). The much enhanced photovoltaic performance of BHJ-SMOSCs based-on ASQAr-1~6 could be attributed to the simultaneously enhanced open-circuit voltage (V_{oc}, 0.81~0.87 V *vs*

0.75 V), short-circuit current density (J_{sc}, 8.07~9.06 mA cm^{-2} *vs* 5.40 mA cm^{-2}), and fill factor (FF, 0.45~0.47 *vs* 0.38) relative to those of the reference ASQB-based device.

1. Introduction

In the past decade, small molecular organic solar cells (SMOSCs) have shown great potential because of their advantages over their polymer counterparts such as well-defined molecular structure and molecular weight, facile material synthesis, and high purity without batch to batch variations,[1-4] while bulk-heterojunction (BHJ) device structure has been demonstrated to be quite effective to obtain high power conversion efficiency (PCE).[5,6] Although the PCE of state-of-the-art BHJ-SMOSCs has already exceeded 9%,[7-9] further enhanced PCE is still needed for practical application, hence much research effort has been devoted into the molecular tailoring of SMOSCs materials bearing similar molecular skeleton, so that the correlations between molecular structure and photovoltaic properties could be revealed, and rational molecular design on high performance SMOSCs materials may be realized. Up to now, some strategies, e.g., the introduction of two-dimensional conjugated side-chain,[7] the fusing of aromatic units through covalent bridging,[10,11] the introduction of cyano groups to the electron-donating subunit,[12] and the incorporation of fused aromatic ring into the molecular skeleton[13] have been demonstrated to be effective for improving the photovoltaic performance of SMOSCs materials. Yet in most cases, just one or two of the three key parameters of SMOSCs (V_{oc}, J_{sc}, and FF) could be enhanced substantially at one time; and only a few molecular tailoring approaches like fluorine-substitution[14] and replacement of furan by thiophene or selenophene[15] have been demonstrated to be effective to enhance V_{oc}, J_{sc} and FF simultaneously. Therefore, it is of great importance to develop more molecular tailoring strategies for the concurrent enhancement of V_{oc}, J_{sc} and FF in SMOSCs, so that satisfactory PCE could be achieved.

Recently, we have exploited an asymmetric squaraines ASQB bearing a *N,N*-diisobutylamino end-capper for photovoltaic applications.[16] Although ASQB displays a relatively low bandgap and good solubility owing to the presence of an electron-rich *N,N*-diisobutylamino group in it, the PCE of the corresponding BHJ-SMOSCs is

unsatisfactory (1.54 %), with low V_{oc} of 0.75 V, J_{sc} of 5.40 mA cm^{-2}, and FF of 0.38. The poor device performance might be ascribed to the relatively high HOMO energy level as well as the electron-insulating isobutyls in ASQB, which should be disadvantageous for obtaining high V_{oc}, J_{sc} and FF.[17,18] Additionally, by replacing the end-capper with a carbazolyl group, the resulting compound ASQC was found to show considerably lowered HOMO energy level, hence ASQC-based SMOSCs displays a very high V_{oc}; however, ASQC exhibits a higher energy bandgap with that of ASQB.[16] Moreover, recent research works have revealed that the replacement of *N*,*N*-alkylamino with *N*,*N*-diarylamino substituents in photovoltaic materials could not only lead to more intensified intermolecular π-π overlap that benefits the broaden of the absorption spectra and the enhancement of charge-transporting properties in film states,[19,20] hence higher J_{sc} could be expected; but also endow these compounds with dropped HOMO energy levels, hence higher V_{oc} could also be expected.[21] Inspired by these discoveries, herein, we designed and synthesized a series of asymmetrical squaraines (ASQAr-1~6) bearing similar molecular skeleton of ASQB, with *N*,*N*-diisobutylamino as end-cappers, and the molecular structure of these objective molecules are shown in Fig. 1. The substituent effects of dialkylamino and diarylamino end-capping groups on the optoelectronic properties of these asymmetric squaraines have been investigated. The results indicated that despite that most of the objective compounds show comparable or even lower hole mobility than that of ASQB, all of the BHJ-SMOSCs using ASQAr-1~6 as electron donor materials show drastically improved photovoltaic performance (PCE: 3.08~3.69%) than the ASQB-based reference device (PCE: 1.54%). It is more exciting that in these ASQAr-based SMOSCs, the three key factors, *i.e.*, V_{oc}, J_{sc}, and FF, were found to be enhanced simultaneously relative to those of the ASQB-based device. To our knowledge, this is one of the most effective molecular design strategies for improving the photovoltaic performance, because the PCE of the corresponding SMOSCs could be increased for over 100%.

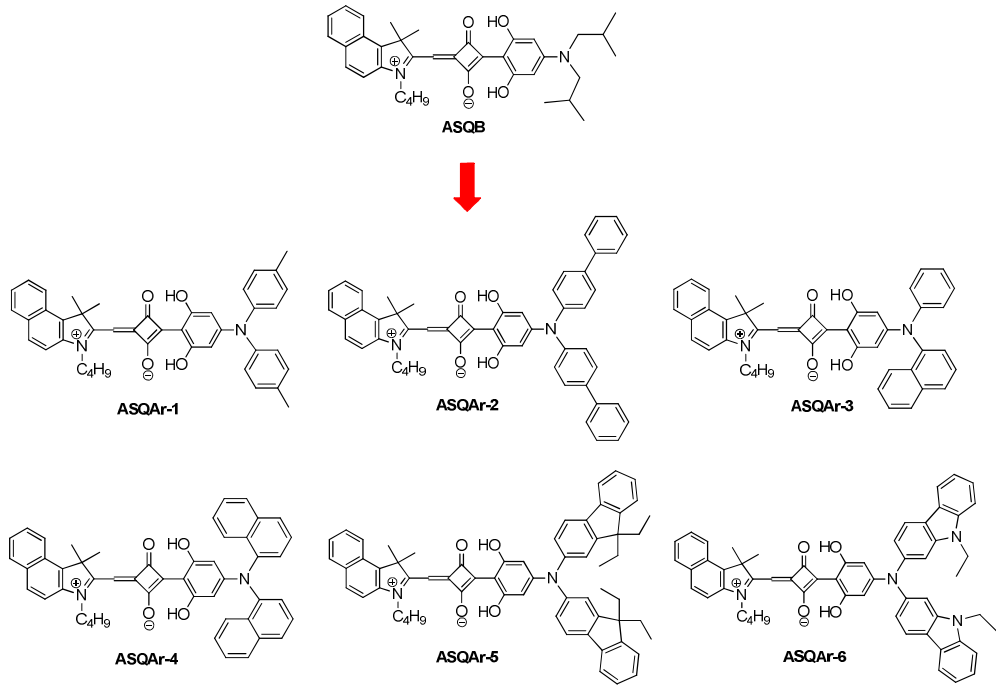

Fig. 1 The molecular structure of the squaraine derivatives.

2. Experimental section

2.1 Instruments and characterization

^{1}H NMR and ^{13}C NMR spectra were measured using a Bruker Avance AV II-400 MHz spectrometer, and the chemical shifts were recorded in units of ppm with TMS as the internal standard. High resolution MS spectra were obtained from a Shimadzu LCMS-IT-TOF. Thermogravimetry analysis (TGA) was performed on a Perkin-Elmer TGA Q500 instrument in an atmosphere of N_2 at a heating rate of 10 °C min^{-1}. The ground-state geometries and electronic structures of these target molecules were calculated with Gaussian 03 software, using density functional theory (DFT) based on B3LYP/6-31G level. Electronic absorption spectra of both solution and thin-film samples of the squaraine derivatives were recorded using a Perkin-Elmer Lamdba 950 UV-Vis scanning spectrophotometer. The solution samples were prepared in chloroform solution at a concentration of 2.00×10^{-6} mol L^{-1}, while the film samples were obtained by spin-coating from chloroform solution (5 mg mL^{-1}, 1400 rpm, 30 s) on quartz substrates. Cyclic voltammetry measurements were carried out in 2.5×10^{-4} mol L^{-1} anhydrous dichloromethane (DCM) with tetrabutyl ammonium bromide (Bu_4NBr) as supporting electrolyte under an Argon atmosphere at a scan rate of 50

mV s^{-1} using a LK 2006A electrochemical workstation. The CV system was constructed using a Pt disk, a Pt wire, and a $Ag/AgNO_3$ (0.1 mol L^{-1} in acetonitrile) electrode as the working electrode, counter electrode and reference electrode, respectively, and the potential of the $Ag/AgNO_3$ reference electrode was internally calibrated with the ferrocene/ ferrocenium redox couple (Fc/Fc^+), which has a known reduction potential of -4.80 eV relative to vacuum level. The morphologies of the active layers were analyzed through atomic force microscopy (AFM) in tapping mode under ambient conditions using a MFP 3D Asylum Research instrument.

2.2 Device Preparation and characterization

Small molecules bulk-heterojunction organic solar cells were fabricated using indium-tin-oxide (ITO) coated glass as substrate. The thickness of ITO is 190 nm and the sheet resistance of ITO is 15 Ω sq^{-1}. The substrate was cleaned consecutively in ultrasonic baths containing detergent, deionized water, acetone and ethanol for 10 min each, and finally blow-dried by high purity nitrogen. The substrate was treated by UV-ozone for 5 min, then immediately transferred into a high vacuum chamber for deposition of 80 Å MoO_3 at pressures of less than 3×10^{-4} Pa with a rate of 0.5 Å s^{-1}. The solution mixtures were stirred for 12 h at room temperature. Subsequently, photoactive layers were fabricated by spin-coating a blend of the target molecules and $PC_{71}BM$ in chloroform with total concentration of 20 mg mL^{-1} (1500 rpm, 30 s) in a N_2-filled glovebox at 25 °C. Then the substrates were loaded into a vacuum chamber to finish the deposit of LiF (8 Å) and Al (1000 Å) at pressures of less than 3×10^{-4} Pa with a rate of 0.05 Å s^{-1} and 1.5 Å s^{-1}, respectively. Deposition rate and film thickness were in situ monitored using a quartz crystal oscillator mounted to the substrate holder. The active area of OPV cells is 6 mm^2. The current-voltage curves under illumination were measured using an Abet solar simulator with a Keithley 4200 source measurement unit under AM 1.5G illumination (100 mW cm^{-2}), after spectral mismatch correction under an ambient atmosphere at 25 °C. The EQE measurements were performed in air using a QE/IPCE Measurements Solar Cell Scan 100 (ZOLIX) system.

2.3 Synthesis

2-Bromo-9,9-diethylfluorene,[22] 2-bromo-9-ethylcarbazole,[23] **7a**[16] and ASQB[16] were prepared according to the procedures described in the literatures. All other chemicals were obtained from commercial sources and used as-received without further purification.

3,5-Dimethoxy-*N*,*N*-di-*p*-tolylaniline (1a).[24] A mixture of 4,4'-dimethyl-diphenylamine (0.91 g, 4.61 mmol), 1-bromo-3,5-dimethoxybenzene (1.00 g, 4.61 mmol), NaOBu-*t* [Sodium *tert*-butoxide] (0.66 g, 6.92 mmol), $Pd(OAc)_2$ [Palladium (II) acetate] (31 mg, 3%), and $P(t\text{-}Bu)_3$ HBF_4 [Tri-*tert*-butyl phosphine tetrafluoroborate] (80 mg, 6%) were dissolved in 50 mL of toluene and refluxed under Ar for 10 h. The reaction mixture was cooled down and filtered to remove insoluble material, then the solvents were removed under reduced pressure. The crude product was purified by silica gel chromatography (eluent: hexane/ dichloromethane = 1/6) to afford **1a** as a white solid (1.00 g, 65%). Mp. 118-119 °C. ^{1}H NMR (400 MHz, $CDCl_3$, δ): 7.06 (d, 4H, *J*=8.4 Hz, Ar-H), 7.00 (d, 4H, *J*=8.4 Hz, Ar-H), 6.16 (d, 2H, ^3J=2.0 Hz, Ar-H), 6.08 (t, 1H, ^3J=2.0 Hz, Ar-H), 3.67 (s, 6H, O-CH_3), 2.30 (s, 6H, -CH_3).

5-(Di-*p*-tolylamino)benzene-1,3-diol (1b). 1a (0.90 g, 2.69 mmol) was dissolved in 30 mL of anhydrous CH_2Cl_2, then boron tribromide (27 mL of 1 M solution in CH_2Cl_2, 26.9 mmol) was added dropwise slowly to it at 0 °C. After the addition was finished, the mixture was stirred at room temperature for 24 h, and then decanted to 120 mL of ice water to remove any excess of BBr_3. The organic phase was separated, and the aqueous phase was extracted with CH_2Cl_2 for three times. The combined organic phases were washed with saturation aqueous $NaHCO_3$ solution and water, dried over anhydrous Na_2SO_4, and then the solvents were removed under reduced pressure. The crude product was purified by silica gel chromatography (eluent: dichloromethane/methanol = 50/1) to afford **1b** as a viscous white solid (0.70 g, 85%).

***N*-([1,1'-biphenyl]-4-yl)-*N*-(3,5-dimethoxyphenyl)-[1,1'-biphenyl]-4-amine (2a).**[21] **2a** was obtained as a white solid (1.21 g, 85%) from the reaction of bis(4-biphenylyl)amine (1.00 g, 3.12 mmol) and 1-bromo-3,5-dimethoxybenzene (0.71 g, 3.27 mmol) according to the procedures described for the synthesis of **1a**. Mp. 134-135 °C. ^{1}H NMR (400 MHz, $CDCl_3$, δ): 7.60 (d, 4H, *J*=8.0 Hz, Ar-H), 7.52 (d, 4H, *J*=8.0 Hz, Ar-H), 7.45 (t, 4H, *J*=8.0 Hz,

Ar-H), 7.34 (t, 2H, *J*=8.0 Hz, Ar-H), 7.22 (d, 4H, *J*=8.0 Hz, Ar-H), 6.32 (d, 2H, ^{3}J=2.0 Hz, Ar-H), 6.20 (t, 1H, ^{3}J=2.0 Hz, Ar-H), 3.73 (s, 6H, O-CH_3).

5-(Di([1,1'-biphenyl]-4-yl)amino)benzene-1,3-diol (2b).[21] **2b** was obtained as a viscous white solid (0.60 g, 64%) from the reaction of **2a** (1.00 g, 2.18 mmol) with boron tribromide (22 mL of 1 M solution in CH_2Cl_2, 21.8 mmol) according to the procedure described for the synthesis of **1b**.

***N*-(3,5-dimethoxyphenyl)-*N*-phenylnaphthalen-1-amine (3a).**[21] **3a** was obtained as a white solid (1.00 g, 61%) from the reaction of *N*-phenyl-1-naphthylamine (1.01 g, 4.61 mmol) with 1-bromo-3,5-dimethoxybenzene (1.00 g, 4.61 mmol) according to the procedure described for the synthesis of **1a**. Mp. 133-134 °C. ^{1}H NMR (400 MHz, $CDCl_3$, δ): 7.95 (d, 1H, *J*=8.4 Hz, Ar-H), 7.87 (d, 1H, *J*=8.0 Hz, Ar-H), 7.77 (d, 1H, *J*=8.4 Hz, Ar-H), 7.47-7.43 (m, 2H, Ar-H), 7.38-7.32 (m, 2H, Ar-H), 7.21 (t, 2H, *J*=8.4 Hz, Ar-H), 7.07 (d, 2H, *J*=7.6 Hz, Ar-H), 6.96 (t, 1H, *J*=7.6 Hz, Ar-H), 6.16 (d, 2H, ^{3}J=2.0 Hz, Ar-H), 6.07 (t, 1H, ^{3}J=2.0 Hz, Ar-H), 3.64 (s, 6H, O-CH_3).

5-(Naphthalen-1-yl(phenyl)amino)benzene-1,3-diol (3b).[21] **3b** was obtained as a pale-yellow viscous solid (0.66 g, 80%) from the reaction of **3a** (0.90 g, 2.53 mmol) with boron tribromide (25 mL of 1 M solution in CH_2Cl_2, 25.3 mmol) according to the procedure described for the synthesis of **1b**.

***N*-(3,5-dimethoxyphenyl)-*N*-(naphthalen-1-yl)naphthalen-1-amine (4a).** A mixture of 1-bromonaphthalene (1.71 g, 8.24 mmol), 3,5-dimethoxyphenylamine (0.60 g, 3.92 mmol), NaOBu-*t* [Sodium *tert*-butoxide] (1.13 g, 11.76 mmol), $Pd(OAc)_2$ [Palladium (II) acetate] (44 mg, 5%), and P(*t*-Bu)$_3$HBF$_4$ [Tri-*tert*-butyl phosphine tetrafluoroborate] (114 mg, 10%) were dissolved in 60 mL of toluene and refluxed under Ar for 12 h. The reaction mixture was cooled down and filtered to remove insoluble material, then the solvents were removed under reduced pressure. The crude product was purified by silica gel chromatography (eluent: hexane/dichloromethane = 5/1) to afford **4a** as a white crystal (0.82 g, 52%). Mp. 185-186 °C. ^{1}H NMR (400 MHz, $CDCl_3$, δ): 8.08 (d, 2H, *J*=8.4 Hz, Ar-H), 7.86 (d, 2H, *J*=8.0 Hz, Ar-H), 7.68 (d, 2H, *J*=8.0 Hz, Ar-H), 7.46 (t, 2H, *J*=8.0, 1.2 Hz, Ar-H), 7.37-7.32 (m, 4H, Ar-H), 7.25 (d, 2H, *J*=7.6 Hz, Ar-H), 6.03 (t, 1H, ^{3}J=2.0 Hz, Ar-H), 5.88 (d, 2H, ^{3}J=2.4 Hz, Ar-H), 3.55 (s, 6H, O-CH_3).

5-(Di(naphthalen-1-yl)amino)benzene-1,3-diol (4b). 4b was obtained as a viscous white solid (0.86 g, 71%) from the reaction of **4a** (1.30 g, 3.19 mmol) with boron tribromide (32 mL of 1 M solution in CH_2Cl_2, 31.90 mmol) according to the procedure described for the synthesis of **1b**.

***N*-(9,9-diethyl-9*H*-fluoren-2-yl)-*N*-(3,5-dimethoxyphenyl)-9,9-diethyl-9*H*-fluoren-2-amine (5a). 5a** was obtained as a white solid (1.98 g, 50%) from the reaction of 2-bromo-9,9-diethylfluorene (4.00 g, 13.29 mmol) with 3,5-dimethoxyphenylamine (1.02 g, 6.65 mmol) according to the procedure described for the synthesis of **4a**. Mp. 97-98 °C. ^{1}H NMR (400 MHz, $CDCl_3$, δ): 7.64 (d, 2H, *J*=7.6 Hz, Ar-H), 7.59 (d, 2H, *J*=8.0 Hz, Ar-H), 7.33-7.27 (m, 6H, Ar-H), 7.14 (d, 2H, ^3J=2.0 Hz, Ar-H), 7.11 (d, 1H, ^3J=1.6 Hz, Ar-H), 7.09 (d, 1H, ^3J=2.0 Hz, Ar-H), 6.29 (d, 2H, ^3J=1.6 Hz, Ar-H), 6.14 (t, 1H, ^3J=2.0 Hz, Ar-H), 3.67 (s, 6H, O-CH_3), 1.99-1.85 (m, 8H, -CH_2), 0.35 (t, 12H, *J*=7.2 Hz, -CH_3).

5-(Bis(9,9-diethyl-9*H*-fluoren-2-yl)amino)benzene-1,3-diol (5b). 5b was obtained as a yellow solid (0.56 g, 59%) from the reaction of **5a** (1.00 g, 1.68 mmol) with boron tribromide (17 mL of 1 M solution in CH_2Cl_2, 16.8 mmol) according to the procedure described for the synthesis of **1b**.

***N*-(3,5-dimethoxyphenyl)-9-ethyl-*N*-(9-ethyl-9*H*-carbazol-2-yl)-9*H*-carbazol-2-amine (6a). 6a** was obtained as a white solid (1.70 g, 69%) from the reaction of 2-bromo-*N*-ethylcarbazole (2.50 g, 9.12 mmol) with 3,5-dimethoxyphenylamine (0.70 g, 4.56 mmol) according to the procedure described for the synthesis of **4a**. Mp. 170-171 °C. ^{1}H NMR (400 MHz, $CDCl_3$, δ): 8.03 (d, 2H, *J*=8.0 Hz, Ar-H), 7.97 (d, 2H, *J*=8.4 Hz, Ar-H), 7.43 (t, 2H, *J*=7.6 Hz, Ar-H), 7.36 (d, 2H, *J*=8.0 Hz, Ar-H), 7.22-7.19 (m, 4H, Ar-H), 7.07 (dd, 2H, *J*=8.4 Hz, Ar-H), 6.35 (d, 2H, ^3J=2.0 Hz, Ar-H), 6.16 (s, 1H, Ar-H), 4.24 (q, 4H, *J*=7.2 Hz, N-CH_2), 3.67 (s, 6H, O-CH_3), 1.34 (t, 6H, *J*=7.2 Hz, -CH_3).

5-(Bis(9-ethyl-9*H*-carbazol-2-yl)amino)benzene-1,3-diol (6b). 6b was obtained as a viscous white solid (0.64 g, 84%) from the reaction of **6a** (0.80 g, 1.48 mmol) with boron tribromide (15 mL of 1 M solution in CH_2Cl_2, 14.8 mmol) according to the procedure described for the synthesis of **1b**.

4-((3-Butyl-1,1-dimethyl-1*H*-benzo[*e*]indol-3-ium-2-yl)methylene)-2-(4-(di-*p*-tolylamino)-2,6-dihydroxyphenyl)-3-oxocyclobut-1-enolate (ASQAr-1). A mixture of **7a** (448 g,

1.24 mmol) and **1b** (379 mg, 1.24 mmol) in *n*-butanol (30 mL) and toluene (30 mL) were added into a round bottom flask. The mixture was refluxed with a Dean-Stark apparatus for 36 h. After the mixture was cooled down, 50 mL methanol was added to the reaction mixture dropwise. The green precipitate was filtered off, and the crude product was collected, purified by silica gel chromatography using dichloromethane/methanol (50:1, v/v) as the eluent to afford green solid. The solid was recrystallized from the mixture of dichloromethane and methanol (1:8, v/v) to afford golden crystals of ASQAr-1 with metallic lustre (645 mg, 80%). Mp. 302-303 °C. ^{1}H NMR (400 MHz, $CDCl_3$, δ):12.25 (s, 2H, -OH), 8.21 (d, 1H, *J*=8.8 Hz, Ar-H), 7.95 (d, 1H, *J*=8.4 Hz, Ar-H), 7.94 (d, 1H, *J*=8.8 Hz, Ar-H), 7.63 (t, 1H, *J*=7.6 Hz, Ar-H), 7.51 (t, 1H, *J*=7.6 Hz, Ar-H), 7.37 (d, 1H, *J*=8.8 Hz, Ar-H), 7.15 (d, 4H, *J*=8.4 Hz, Ar-H), 7.10 (d, 4H, *J*=8.4 Hz, Ar-H), 5.94 (s, 1H, -CH-), 5.87 (s, 2H, Ar-H), 4.20 (t, 2H, *J*=7.6 Hz, N-CH_2), 2.34 (s, 6H, -CH_3), 2.01 (s, 6H, -CH_3), 1.90-1.80 (m, 2H, -CH_2-), 1.53-1.47 (m, 2H, -CH_2-), 1.03 (t, 3H, *J*=7.2 Hz, -CH_3); ^{13}C NMR (100 MHz, $CDCl_3$, δ): 175.0, 169.4, 169.0, 157.6, 142.5, 138.7, 135.9, 135.8, 132.0, 130.2, 129.8, 128.8, 127.8, 127.3, 125.4, 122.7, 110.4, 104.4, 98.3, 87.3, 52.0, 44.4, 29.7, 26.4, 21.0, 20.3, 13.8. HR-MS (ESI): *m/z* $[M + H]^+$ calcd. for $C_{43}H_{40}N_2O_4$: 649.3066; found: 649.3062.

4-((3-Butyl-1,1-dimethyl-1*H*-benzo[*e*]indol-3-ium-2-yl)methylene)-2-(4-(di([1,1'-biphenyl]-4-yl)amino)-2,6-dihydroxyphenyl)-3-oxocyclobut-1-enolate (ASQAr-2). ASQAr-2 was obtained from the reaction of **7a** (444 mg, 1.23 mmol) with **2b** (590 mg, 1.37 mmol) according to the procedure described for the synthesis of ASQAr-1. The solid was recrystallized from the mixture of dichloromethane and methanol (1:8, v/v) to afford golden crystals of ASQAr-2 with metallic lustre (750 mg, 79%). Mp. 276-277 °C. ^{1}H NMR (400 MHz, $CDCl_3$, δ): 12.15 (s, 2H, -OH), 8.23 (d, 1H, *J*=8.8 Hz, Ar-H), 7.96 (dd, 2H, *J*=8.8 Hz, Ar-H), 7.65-7.57 (m, 9H, Ar-H), 7.53 (t, 1H, *J*=8.0 Hz, Ar-H), 7.48 (t, 4H, *J*=8.0 Hz, Ar-H), 7.40-7.34 (m, 3H, Ar-H), 7.31 (d, 4H, *J*=8.4 Hz, Ar-H), 6.05 (s, 2H, Ar-H), 6.00 (s, 1H, -CH-), 4.25 (t, 2H, *J*=7.6 Hz, N-CH_2), 2.03 (s, 6H, -CH_3), 1.92-1.84 (m, 2H, -CH_2-), 1.56-1.46 (m, 2H, -CH_2-), 1.04 (t, 3H, *J*=7.2 Hz, -CH_3); ^{13}C NMR (100 MHz, $CDCl_3$, δ): 175.7, 170.2, 169.1, 162.5, 156.7, 144.4, 140.3, 138.6, 136.2, 132.1, 130.3, 129.8, 128.8, 128.3, 128.2, 127.9, 127.5, 127.3, 127.0, 125.6, 122.8, 110.5, 104.5, 99.6, 87.8, 52.3, 44.5, 29.8, 26.4, 20.3, 13.8; HR-MS (ESI): *m/z* $[M + H]^+$ calcd. for $C_{53}H_{44}N_2O_4$: 773.3373; found:

773.3379.

4-((3-Butyl-1,1-dimethyl-1*H*-benzo[*e*]indol-3-ium-2-yl)methylene)-2-(2,6-dihydroxy-4-(naphthalen-1-yl(phenyl)amino)phenyl)-3-oxocyclobut-1-enolate (ASQAr-3). ASQAr-3 was obtained from the reaction of **7a** (440 mg, 1.22 mmol) with **3b** (400 mg, 1.22 mmol) according to the procedure described for the synthesis of ASQAr-1. The solid was recrystallized from the mixture of dichloromethane and methanol (1:6, v/v) to afford golden crystals of ASQAr-3 with metallic lustre (663 mg, 81%). Mp. 274-275 °C. ^{1}H NMR (400 MHz, $CDCl_3$, δ): 12.24 (s, 2H, -OH), 8.21 (d, 1H, *J*=8.4 Hz, Ar-H), 7.95-7.89 (m, 4H, Ar-H), 7.84 (d, 1H, *J*=8.4 Hz, Ar-H), 7.63 (t, 1H, *J*=7.6 Hz, Ar-H), 7.52-7.45 (m, 4H, Ar-H), 7.40 (t, 2H, *J*=8.8 Hz, Ar-H), 7.30-7.29 (m, 4H, Ar-H), 7.16-7.12 (m, 1H, Ar-H), 5.95 (s, 1H, -CH-), 5.83 (s, 2H, Ar-H), 4.21 (t, 2H, *J*=7.2 Hz, N-CH_2), 2.00 (s, 6H, -CH_3), 1.90-1.82 (m, 2H, -CH_2-), 1.54-1.44 (m, 2H, -CH_2-), 1.03 (t, 3H, *J*=7.2 Hz, -CH_3); ^{13}C NMR (100 MHz, $CDCl_3$, δ): 175.5, 169.8, 169.4, 157.8, 145.3, 141.1, 138.6, 136.0, 135.1, 132.0, 131.1, 130.3, 129.8, 129.4, 128.5, 128.3, 128.1, 127.8, 127.6, 127.2, 126.5, 126.1, 126.0, 125.5, 125.5, 123.6, 122.8, 110.5, 104.4, 98.3, 87.5, 52.2, 44.5, 29.8, 26.4, 20.3, 13.8. HR-MS (ESI): *m/z* $[M + H]^+$ calcd. for $C_{45}H_{38}N_2O_4$: 671.2910; found: 671.2908.

4-((3-Butyl-1,1-dimethyl-1*H*-benzo[*e*]indol-3-ium-2-yl)methylene)-2-(4-(di(naphthalen-1-yl)amino)-2,6-dihydroxyphenyl)-3-oxocyclobut-1-enolate (ASQAr-4). ASQAr-4 was obtained from the reaction of **7a** (686 mg, 1.90 mmol) and **4b** (800 mg, 2.11 mmol) according to the procedure described for the synthesis of ASQAr-1. The solid was recrystallized from a 1:6 volume ratio of dichloromethane and methanol mixture to afford green crystals of ASQAr-4 with metallic lustre (1114 mg, 81%). Mp. 222-223 °C. ^{1}H NMR (400 MHz, $CDCl_3$, δ): 8.20 (d, 1H, *J*=8.8 Hz, Ar-H), 8.12 (br, 2H, Ar-H), 7.95-7.90 (m, 4H, Ar-H), 7.79 (d, 2H, *J*=8.0 Hz, Ar-H), 7.62-7.47 (m, 6H, Ar-H), 7.42 (d, 2H, *J*=7.2 Hz, Ar-H), 7.37-7.34 (m, 3H, Ar-H), 5.94 (s, 1H, -CH-), 5.58 (s, 2H, Ar-H), 4.20 (t, 2H, *J*=7.2 Hz, N-CH_2), 1.99 (s, 6H, -CH_3), 1.89-1.81 (m, 2H, -CH_2-), 1.53-1.44 (m, 2H, -CH_2-), 1.02 (t, 3H, *J*=7.2 Hz, -CH_3); ^{13}C NMR (100 MHz, $CDCl_3$, δ): 175.3, 169.6, 169.4, 158.8, 141.6, 138.6, 135.9, 135.1, 132.0, 130.5, 130.2, 129.8, 128.6, 128.2, 127.8, 127.2, 126.4, 126.0, 125.7, 125.5, 124.0, 122.7, 110.4, 97.1, 87.4, 52.1, 44.4, 29.7, 26.3, 20.3, 13.8. HR-MS (ESI): *m/z* $[M + H]^+$ calcd. for $C_{49}H_{40}N_2O_4$: 721.3066; found: 721.3059.

2-(4-(Bis(9,9-diethyl-9*H*-fluoren-2-yl)amino)-2,6-dihydroxyphenyl)-4-((3-butyl-1,1-dimethyl-1*H*-benzo[*e*]indol-3-ium-2-yl)methylene)-3-oxocyclobut-1-enolate (ASQAr-5). ASQAr-5 was obtained from the reaction of **7a** (340 mg, 0.94 mmol) and **5b** (560 mg, 0.99 mmol) according to the procedure described for the synthesis of ASQAr-1. The solid was recrystallized from a 1:10 volume ratio of dichloromethane and methanol mixture to afford green crystals of ASQAr-5 (690 mg, 81%). Mp. 270-271 °C. ^{1}H NMR (400 MHz, $CDCl_3$, δ): 12.26 (s, 2H, -OH), 8.21 (d, 1H, *J*=8.4 Hz, Ar-H), 7.96 (d, 1H, *J*=8.0 Hz, Ar-H), 7.95 (d, 1H, *J*=8.8 Hz, Ar-H), 7.87 (d, 4H, *J*=8.0 Hz, Ar-H), 7.63 (t, 1H, *J*=7.2 Hz, Ar-H), 7.52 (t, 1H, *J*=7.2 Hz, Ar-H), 7.38-7.27 (m, 9H, Ar-H), 7.11 (d, 2H, ^{3}J=1.2 Hz, Ar-H), 6.07 (s, 2H, Ar-H), 5.98 (s, 1H, -CH-), 4.23 (t, 2H, *J*=7.6 Hz, N-CH_2), 2.03 (s, 6H, -CH_3), 2.00-1.84 (m, 10H, -CH_2-), 1.55-1.46 (m, 3H, -CH_2-), 1.04 (t, 3H, *J*=7.2 Hz, -CH_3), 0.34 (t, 12H, *J*=7.2 Hz, -CH_3); ^{13}C NMR (100 MHz, $CDCl_3$, δ): 175.4, 169.5, 169.0, 157.2, 151.5, 150.1, 144.7, 140.9, 139.2, 138.7, 136.0, 132.0, 130.3, 129.9, 128.3, 127.9, 127.0, 126.0, 125.5, 122.8, 122.8, 121.5, 120.4, 119.6, 110.5, 104.9, 99.8, 87.7, 56.2, 52.2, 44.5, 32.7, 29.8, 26.4, 20.3, 13.9, 8.6. HR-MS (ESI): *m/z* $[M + H]^+$ calcd. for $C_{463}H_{60}N_2O_4$: 909.4631; found: 909.4638.

2-(4-(Bis(9-ethyl-9*H*-carbazol-2-yl)amino)-2,6-dihydroxyphenyl)-4-((3-butyl-1,1-dimethyl-1*H*-benzo[*e*]indol-3-ium-2-yl)methylene)-3-oxocyclobut-1-enolate (ASQAr-6). ASQAr-6 was obtained from the reaction of **7a** (470 mg, 1.30 mmol) and **6b** (740 mg, 1.45 mmol) according to the procedure described for the synthesis of ASQAr-1. The solid was recrystallized from a 1:12 volume ratio of dichloromethane and methanol mixture to afford red crystals of ASQAr-6 (530 mg, 62%). Mp. 280-281 °C. ^{1}H NMR (400 MHz, $CDCl_3$, δ): 8.20 (d, 1H, *J*=8.8 Hz, Ar-H), 8.07 (t, 4H, *J*=8.4 Hz, Ar-H), 7.95-7.92 (m, 2H, A-rH), 7.63 (t, 1H, *J*=8.0 Hz, Ar-H), 7.51-7.35 (m, 6H, Ar-H), 7.31 (s, 2H, Ar-H), 7.25 (t, 2H, *J*=7.2 Hz, Ar-H), 7.15 (d, 2H, *J*=8.0 Hz, Ar-H), 6.09 (s, 2H, Ar-H), 5.99 (s, 1H, -CH-), 4.30 (q, 4H, *J*=6.8 Hz, N-CH_2), 4.21 (t, 2H, *J*=7.2 Hz, N-CH_2), 2.02 (s, 6H, -CH_3), 1.90-1.83 (m, 2H, -CH_2-), 1.53-1.45 (m, 2H, -CH_2-), 1.40 (t, 6H, *J*=7.2 Hz, -CH_3), 1.03 (t, 3H, *J*=7.2 Hz, -CH_3); ^{13}C NMR (100 MHz, $CDCl_3$, δ): 175.1, 169.3, 169.2, 158.0, 143.5, 140.6, 140.6, 138.7, 135.9, 132.0, 130.2, 129.8, 128.3, 127.8, 125.6, 125.4, 122.7, 122.6, 121.1, 120.9, 120.3, 119.2, 118.8, 110.4, 108.5, 107.4, 104.8, 99.5, 87.5, 52.1, 44.4, 37.6, 29.8, 26.4, 20.3, 13.8. HR-MS (ESI): *m/z* $[M + H]^+$ calcd. for $C_{57}H_{50}N_4O_4$: 854.3910; found: 855.3914.

3. Results and Discussion

3.1 Synthesis and characterization

The synthetic routes to the target molecules are illustrated in Scheme 1. *N,N*-diaryl-3,5-dimethoxyanilines (**1a**~**6a**) were prepared by Buchwald-Hartwig reaction using 1-bromo-3,5-dimethoxybenzene and appropriate diarylamines or 3,5-dimethoxyaniline and appropriate aryl bromides as reactants. The methoxy groups of **1a**~**6a** were deprotected in the presence of BBr_3 to afford 5-(diarylamino)benzene-1,3-diol (**1b**~**6b**), so that they could condense with the benzo[*e*]indole-modified semi-squarylium compound **7a** to obtain the target molecules ASQAr-1~6 with yields of up to 80%. The molecular structures of the target molecules were confirmed by ^{1}H NMR, ^{13}C NMR and HR-MS. All the six target molecules show good solubility in common organic solvents like chloroform, chlorobenzene and 1,2-dichlorobenzene. Additionally, high quality thin solid films of the target molecules could be obtained through spin-coating from solution, suggesting that they are very suitable for solution-processing.[25] As shown in Fig. 2, all the target molecules display higher decomposition temperature than that of ASQB (data summarized in Table 1), confirming that the *N,N*-diarylamino end-capping groups could endow squaraine dyes with enhanced thermal stability.

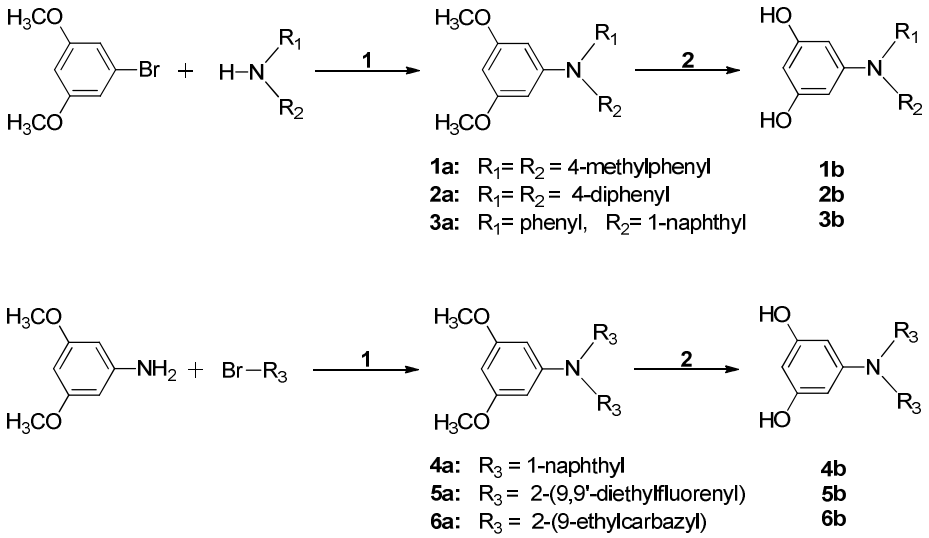

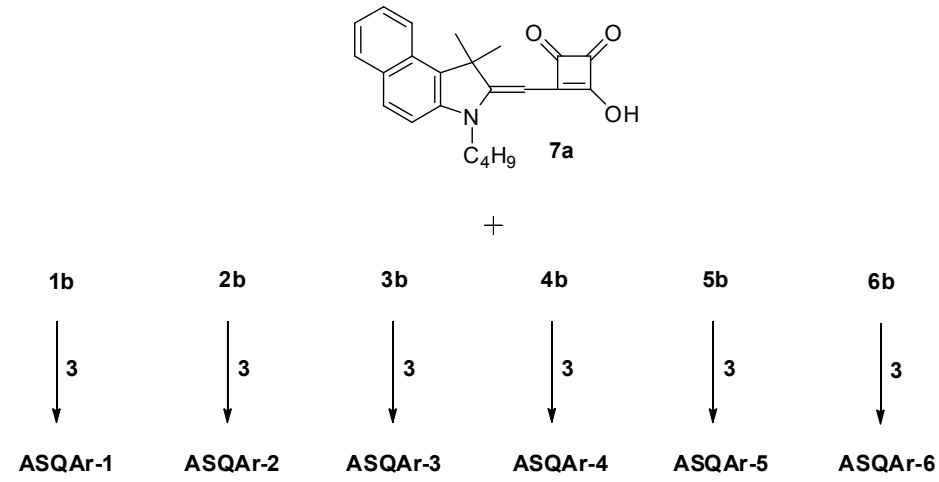

Scheme 1. Synthetic routes to the target molecules ASQAr-1~6. Reaction conditions: 1. NaOBu-*t*, $Pd(OAc)_2$, P(*t*-Bu)$_3$ HBF_4, toluene, reflux 10 h; 2. BBr_3, dichloromethane, room temperature, 24 h; 3. *n*-Butanol and toluene (1:1), 140 °C, 36 h.

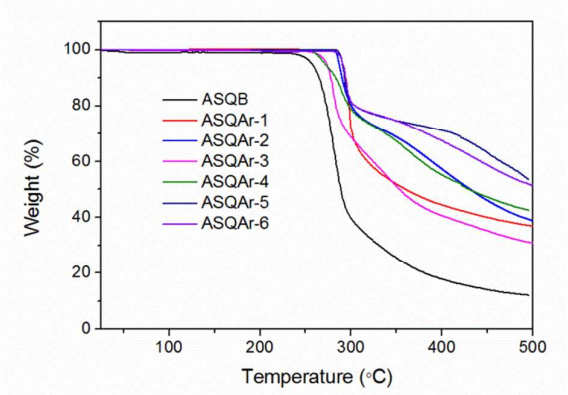

Fig. 2 TGA curves of the squaraine derivatives.

3.2 Optical properties

The UV-Vis absorption spectra of these squaraine derivatives in solution and thin film states are shown in Fig. 3, and data are summarized in Table 1. In chloroform solution, ASQB has an absorption band with λ_{max} of 656 nm and full width half maxima (FWHM) of 25 nm. While the target compounds ASQAr-1~6 bearing diarylamino end-cappers all display red-shifted and broadened absorption bands ,with λ_{max} of 659~686 nm and FWHM of 34~66 nm, indicating that the aryl segments of the end-capping groups contribute to the extension

of the π-conjugation system of these compounds. In thin film states, the absorption spectrum of ASQB is bathochromic-shifted for 42 nm (λ_{max}: 698 nm) and broadened for 98 nm (FWHM: 123 nm) compared with that of the solution sample; while ASQAr-1~6 show 21~31 nm red-shifted and 72~100 nm widened absorption bands, with λ_{max} of 688~709 nm and FWHM of 127~150 nm. The optical bandgaps of ASQAr-1~6 were determined to be 1.44~1.54 eV, are lower than that of the reference compound ASQB (1.55 eV). Consequently, the alteration of the end-capping subunit from diisobutylamino to diarylamino groups could render compounds with both lowered energy bandgaps and broadened absorption bands, which are propitious to the enhancement of J_{sc} in photovoltaic devices. Yet despite that in condensed state, ASQAr-1~6 all show considerable bathochromic-shifted and widened absorption spectra than that in dilute solution, the extent of the spectral red-shift and breadth of ASQAr-1~6 is just comparable or even less than that of ASQB, implying that the intermolecular π-π stacking interactions within these ASQAr compounds may be comparable or even less than those within ASQB, which maybe result in lower mobilities for ASQAr-1~6 .

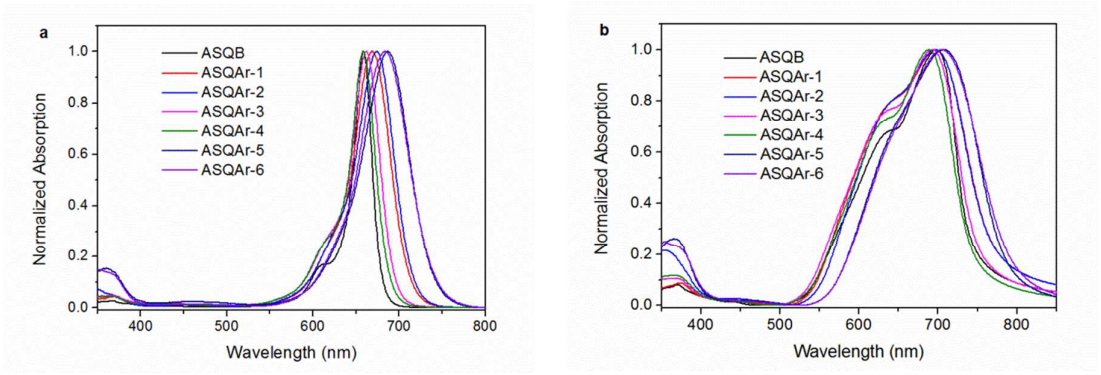

Fig. 3 Absorption spectra of the squaraine derivatives in (a) chloroform solution, and (b) thin film.

Table 1. Optical and electrochemical properties of the squaraine derivatives .

Compound	Absorption	λ_{max} (nm)	FWHM (nm)		E_g^{opt}	T_d
	Solution	Film	Solution	Film	eV	°C
ASQB	656	698, 637	25	123	1.55	257
ASQAr-1	667	698, 636	50	150	1.49	290

ASQAr-2	674	698, 636	52	146	1.49	287
ASQAr-3	661	692, 634	39	138	1.52	273
ASQAr-4	659	688, 629	34	127	1.54	271
ASQAr-5	686	709	65	138	1.46	290
ASQAr-6	684	705	66	138	1.44	291

3.3 Electrochemistry properties

To estimate the energy levels of the HOMO/LUMO of the compounds, cyclic voltammetry (CV) measurement has been carried out (voltammograms shown in Fig. S1; data summarized in Table 2), and the data were transformed into frontier molecular orbital (FMO) energy levels *vs.* vacuum (shown in Fig. 4). As the redox potential of Fc/Fc^+ is considered to have an absolute energy level of –4.80 eV relative to vacuum,[26] the HOMO of the these compounds are calculated according to the following equations:

$$\text{HOMO} = -\,[E_{ox} + 4.80\,]$$

where E_{ox} is the onset oxidation potential *vs.* $Ag/AgNO_3$. During the anodic scan, all these squaraine derivatives exhibit two-electron oxidation signals, and the first signal is reversible. Accordingly, the HOMO energy levels of these compounds were calculated to be –5.16~ –5.04 eV. In comparison with ASQB, all the six target molecules possess deeper (0.04~0.12 eV) HOMO energy levels, which may be attributed to the weaker electron-donating capability of diarylamino relative to dialkylamino groups. Therefore, higher V_{oc} could be expected when ASQAr-1~6 were used as photovoltaic electron-donors instead of ASQB to fabricate SMOSCs.[27] As no reduction wave could be detected due to the limited range available in CH_2Cl_2, the LUMO energy levels of ASQAr-1~6 were deduced from their HOMO energy levels and corresponding optical bandgaps,[28] and were calculated to be –3.65~ –3.60 eV, which is lower 0.10~0.14 eV than that of ASQB.

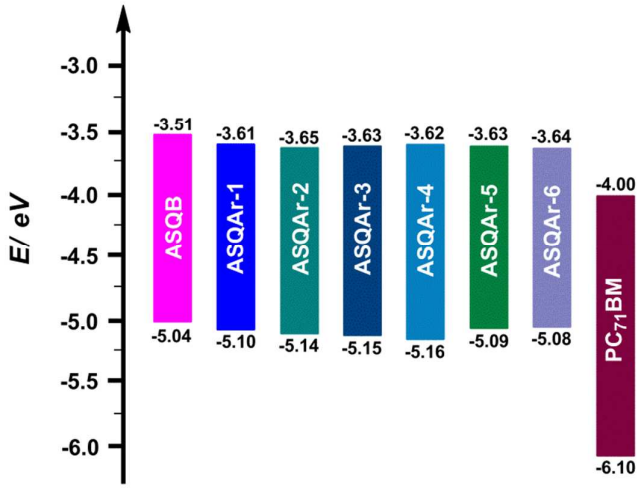

Fig. 4 FMO energy levels of the squaraine derivatives and $PC_{71}BM$.[29]

3.4 DFT calculations

To gain further insights into the effects of the end-capping groups on the electronic properties of theses squaraine compounds, quantum chemical DFT calculations were performed, and the electron density distribution of the HOMO and LUMO of these molecules are shown in Fig. 5. The HOMO and LUMO of ASQB have similar electronic structures, with their electron density delocalized predominantly on the π-conjugation skeleton rather than the isobutyl segments. Consequently, the HOMO→LUMO transition of ASQB should possess $\pi\pi^*$ character, leading to a relative narrow absorption band.[30,31] Yet for ASQAr-1~6, their HOMOs are not only delocalized on the molecular skeleton, but also on the aryl groups of the end-cappers; while their LUMOs are mainly localized on the molecular backbone. Hence the HOMO→LUMO excitation of ASQAr-1~6 should contain a major part of $\pi\pi^*$-featured transition together with some contribution of CT transition from the end-capping aryls to the skeleton. This transition feature could account for the more red-shifted and broadened absorption spectra of the target compounds.[31] In addition, as shown in Table 2, the HOMO energy levels of ASQAr-1~6 were calculated to be –5.27~ –5.19 eV, which well reproduce their corresponding experimental values (–5.16~ –5.08 eV); in addition, the HOMO energy levels of the objective compounds were calculated to be lower than that of ASQB (–5.15 eV). All these calculation results are consistent with the experimental results, indicating that these computational results are reliable.

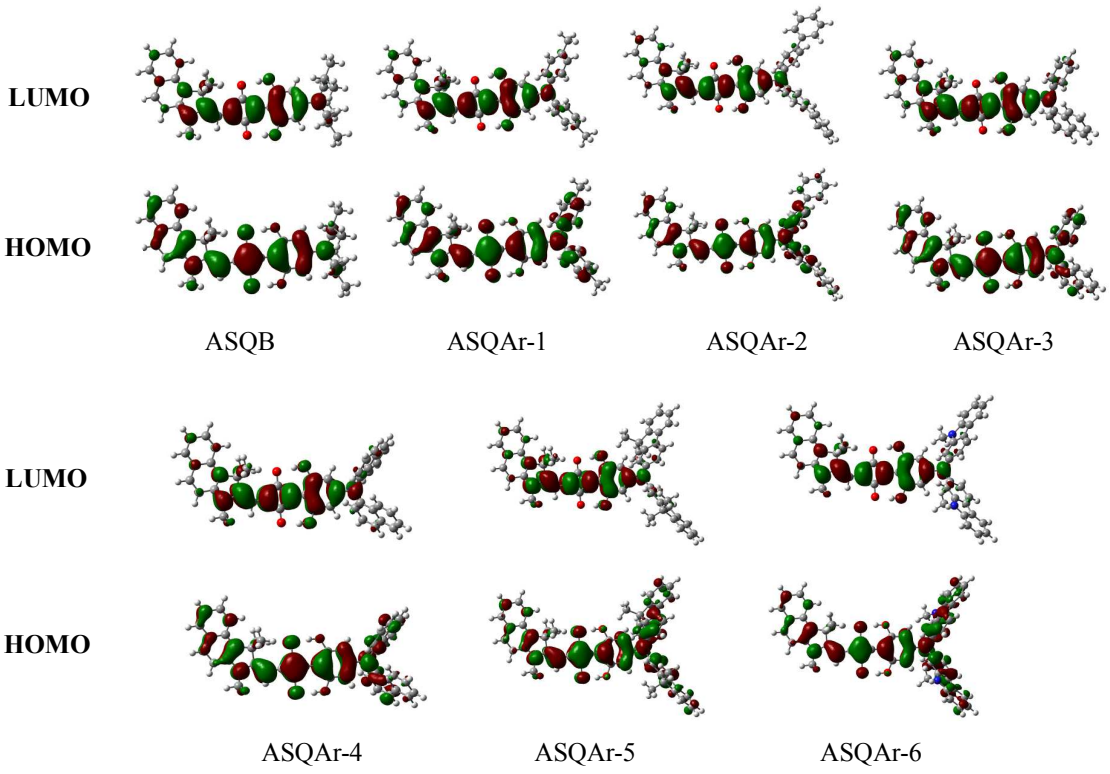

Fig. 5 The electron density distribution of the squaraine derivatives.

Table 2. Cyclic voltammetry data and calculated energy levels for the squaraine derivatives.

Compound	E_{ox}^{onest} (V)	HOMO [a] (eV)	LUMO [b] (eV)	HOMO [c] (eV)	LUMO [c] (eV)	E_g [c] (eV)
ASQB	0.24	–5.04	–3.51	–5.15	–2.85	2.30
ASQAr-1	0.30	–5.10	–3.61	–5.21	–3.03	2.18
ASQAr-2	0.34	–5.14	–3.65	–5.25	–3.07	2.18
ASQAr-3	0.35	–5.15	–3.63	–5.26	–3.04	2.22
ASQAr-4	0.36	–5.16	–3.62	–5.27	–3.05	2.22
ASQAr-5	0.29	–5.09	–3.63	–5.20	–3.05	2.15
ASQAr-6	0.28	–5.08	–3.64	–5.19	–3.04	2.15

[a] HOMO values derived from CV measurements; [b] LUMO = E_g + HOMO; [c] data derived from DFT calculations.

3.5 Hole mobility

The hole transporting property of these squaraine donor materials and the donor/$PC_{71}BM$

composite films (1:5, wt%) were evaluated by the space charge limited current (SCLC) method, and the hole-only device structure is ITO/ MoO_3 (80 Å)/ active layer (800 Å)/ Au (1000 Å).[29] As show in Fig. 6 and Table 3, the hole mobility of the neat ASQB film is 3.19 × 10^{-5} cm^2 V s^{-1}; and that of the ASQB/$PC_{71}BM$ composite film is 1.34 × 10^{-5} cm^2 V s^{-1}. While for the six objective compounds, the hole mobility of their neat films were calculated to be 0.56 × 10^{-5}~5.42 × 10^{-5} cm^2 V s^{-1}, and that of the composite films is 0.44 × 10^{-5}~1.77 × 10^{-5} cm^2 V s^{-1}, both are comparable or even lower than that of ASQB samples. It is noted that these carrier mobility experimental results seems to be contradictory to some literature reports that the alteration of dialkylamino substituents into diarylamino ones could result in photovoltaic compounds with improved charge transporting properties.[19-21] Therefore, for these asymmetrical squaraine derivatives, the presence of *N,N*-diarylamino end-cappers could not endow them with better hole mobility. This result should be of great importance for the recognition of the role *N,N*-diarylamino substituents might play in rational molecular design of photovoltaic compounds.

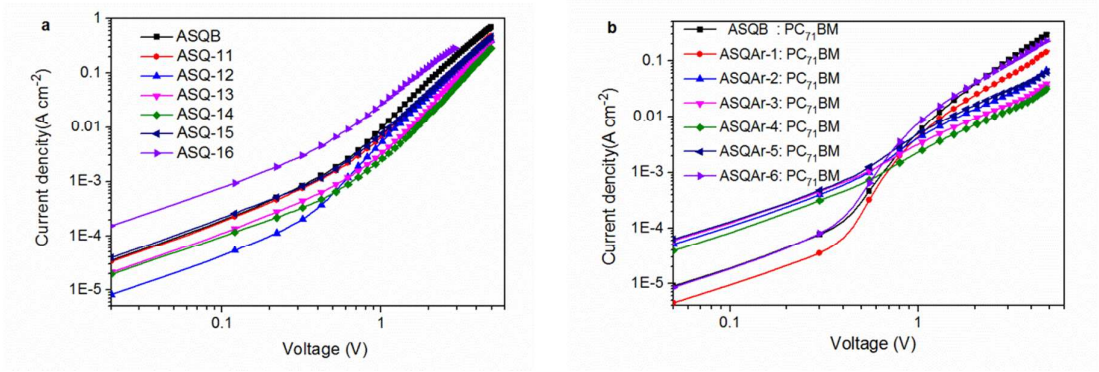

Fig. 6 *J-V* characteristic of the hole-only devices using (a) the neat film of the squaraine donors, and (b) the donor/ $PC_{71}BM$ (1:5, wt%) composite film as active layer.

3.6 BHJ solar cells

To investigate the effects that different end-cappers like dialkylamino and diarylamino groups would have on the photovoltaic properties of their corresponding squaraine dyes, BHJ-SMOSCs using ASQAr1~6 as electron donors were fabricated with the very similar device structure of the ASQB-based device we fabricated before (glass/ ITO/ MoO_3 (80 Å)/

ASQ: $PC_{71}BM$ (1:5, 800 Å)/ LiF (8 Å)/ Al (1000 Å)).[16] The *J-V* curves of the devices are illustrated in Fig. 7a, and some representative data are summarized in Table 3.

Obviously, the PCEs of all the devices using ASQAr-1~6 as electron donors (3.08~3.69%) are significantly (over 100%) higher than that of the ASQB-based reference device (1.54%). More excitingly, compared to the reference device, the three key photovoltaic factors of these ASQAr-based SMOSCs, *i.e.*, V_{oc}, J_{sc}, and FF, were found to be enhanced simultaneously. In detail, the V_{oc} of the ASQAr-based devices is 0.06~0.12 V higher than that of the reference device; the J_{sc} of the ASQAr-based devices is 8.07~9.06 mA cm^{-2}, which is much higher than that of the reference device (5.40 mA cm^{-2}); and the FF of the ASQAr-based devices is ~0.08 higher than that of the reference device. The much elevated V_{oc} of 0.06~0.12 V in the ASQAr-based devices should be safely attributed to the deeper (0.04~0.12 eV) HOMO energy levels of ASQArs. As J_{sc} correlate highly not only with the charge carrier mobility of the electron donor and acceptor, but also with the light-harvesting capability, the charge separation efficiency, as well as the morphology of the donor-acceptor blending films.[33-35] To gain insights into the reason for the drastically increased J_{sc} in ASQAr-based devices, we investigated the EQE curves of these devices firstly. As shown in Fig. 7b, consistent with their absorption properties, devices based on ASQAr-1~6 show more broadened spectral response in 700-800 nm than the reference device based on ASQB, implying that the broader absorption band of ASQArs relative to ASQB indeed contributes to the light-harvesting hence the enhancement of J_{sc}. Nevertheless, in the spectral region of 350-750 nm, the EQE values of ASQAr-devices were observed to be much higher than that of the reference device, hence the enhanced performance of these devices should not just be attributed to the broadened absorption bands of the objective compounds. Since morphological property of the photoactive films is another factor affecting the J_{sc} and FF of the devices, AFM characterizations have been carried out on the ASQ/$PC_{71}BM$ (1:5, wt%) blending films (show in Fig. S2). However, the results indicated that the composite films with ASQB or ASQAr-1~6 as donor all show similar morphologies and quite smooth surfaces with root-mean-square (RMS) of 0.21~0.29 nm. Taking into consideration that the aryl groups of the diarylamino end-capper are more electron-conductive than that of diisobutyl ones, and the aryl groups contribute effectively to the HOMO and LUMO of

ASQAr-1~6, thus, we suppose that more efficient charge separation would occur at the interface of ASQAr/$PC_{71}BM$ than that of ASQB/$PC_{71}BM$, which is beneficial to the increased J_{sc} of the ASQAr-devices.[16,36] And further investigations are still under way to reveal the origin of the enhanced J_{sc} and FF in these devices.

Table 3. The photovoltaic performances of organic solar cells based on ASQs: $PC_{71}BM$.

Active layer	V_{oc} (V)	J_{sc} (mA cm^{-2})	FF	PCE (%)	μ_h [a] (cm^2 v^{-1} s^{-1})	μ_h [b] (cm^2 v^{-1} s^{-1})
ASQB : $PC_{71}BM$	0.75	5.40	0.38	1.54	3.19×10^{-5}	1.34×10^{-5}
ASQAr-1 : $PC_{71}BM$	0.83	9.06	0.47	3.53	1.11×10^{-5}	1.09×10^{-5}
ASQAr-2 : $PC_{71}BM$	0.87	9.02	0.47	3.69	1.21×10^{-5}	0.77×10^{-5}
ASQAr-3 : $PC_{71}BM$	0.87	8.46	0.45	3.31	0.57×10^{-5}	0.60×10^{-5}
ASQAr-4 : $PC_{71}BM$	0.87	8.23	0.45	3.22	0.56×10^{-5}	0.44×10^{-5}
ASQAr-5 : $PC_{71}BM$	0.85	9.03	0.46	3.53	1.33×10^{-5}	1.05×10^{-5}
ASQAr-6 : $PC_{71}BM$	0.81	8.07	0.47	3.08	5.42×10^{-5}	1.77×10^{-5}

[a] Hole mobility of the neat donor films; [b] hole mobility of the donor/$PC_{71}BM$ (1:5, wt%) blending films.

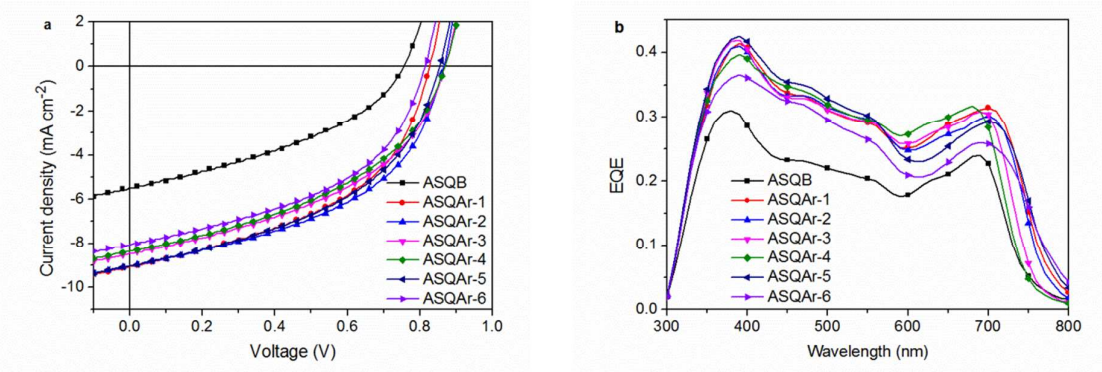

Fig. 7 (a) *J-V* curve characteristics, and (b) EQE curves of the photovoltaic devices.

4. Conclusion

A series of new asymmetrical squaraines bearing an *N,N*-diarylamino end-capper, namely ASQAr-1~6, were designed and synthesized. Compared to the reference compound ASQB

with a *N,N*-diisobutylamino end-capper, ASQAr-1~6 were found to show red-shifted and broadened absorption bands, better thermal stability, lower HOMO and LUMO energy levels, as well as comparable solubility. Despite the fact that the hole mobility of most of the objective compounds is lower than that of ASQB, BHJ-SMOSCs using ASQAr-1~6 as electron donors show simultaneously improved V_{oc}, J_{sc} and FF compared with the reference ASQB-device, and the PCEs of these devices has been increased for over 100% (3.08~3.69% *vs.* 1.54%). These preliminary works demonstrate that *N,N*-diarylamino end-capping may pave a very important strategy for simultaneous enhancement of V_{oc}, J_{sc} and FF, resulting in high PCE in SMOSCs.

Acknowledgements

We acknowledge the financial support for this work by the National Natural Science Foundation of China (project No. 21372168, 21190031 and 21432005), the Research Fund for the Doctoral Program of Higher Education (project No. 20120009130005) and China Scholarship Council. We are grateful to Comprehensive Training Platform of Specialized Laboratory, College of Chemistry, Sichuan University for providing NMR and HR-MS for the intermediates and objective molecules.

References

1 Y. Lin, Y. Li and X. Zhan, *Chem. Soc. Rev.*, 2012, **41**, 4245-4272.

2 A. Mishra and P. Bäuerle, *Angew. Chem. Int. Ed.*, 2012, **51**, 2020-2067.

3 J. Roncali, P. Leriche and P. Blanchard, *Adv. Mater.*, 2014, **26**, 3821-3838.

4 W. Ni, M. Li, X. Wan, H. Feng, B. Kan, Y. Zuo and Y. Chen, *RSC Adv.*, 2014, **4**, 31977-31980.

5 Y. Sun, G. C. Welch, W. L. Leong, C. J. Takacs, G. C. Bazan and A. J. Heeger, *Nat. Mater.,* 2012, **11**, 44-48.

6 Y. Huang, E. J. Kramer, A. J. Heeger and G. C. Bazan, *Chem. Rev.*, 2014, **114**, 7006-7043.

7 V. Gupta, A. K. K. Kyaw, D. H. Wang, S. Chand, G. C. Bazan and A. J. Heeger, *Sci. Rep.*, 2013, **3**, 1965.

8. Q. Zhang, B. Kan, F. Liu, G. Long, X. Wan, X. Chen, Y. Zuo, W. Ni, H. Zhang, M. Li, Z. Hu, F. Huang, Y. Cao, Z. Liang, M. Zhang, T. P. Russell and Y. Chen, *Nat. Photon.*, 2015, **9**, 35-41..

9. B. Kan, Q. Zhang, M. Li, X. Wan, W. Ni, G. Long, Y. Wang, X. Yang, H. Feng and Y. Chen, *J. Am. Chem. Soc.*, 2014, **136**, 15529-15532.

10 D. Demeter, V. Jeux, P. Leriche, P. Blanchard, Y. Olivier, J. Cornil, R. Po and J. Roncali, *Adv. Funct. Mater.*, 2013, **23**, 4854-4861.

11 S. Paek, N. Cho, S. Cho, J. K. Lee and J. Ko, *Org. Lett.*, 2012, **14**, 6326-6329.

12 S. Zeng, L. Yin, C. Ji, X. Jiang, K. Li, Y. Li and Y. Wang, *Chem. Commun.*, 2012, **48**, 10627-10629.

13 Y. S. Choi and W. H. Jo, *Org. Electron.*, 2013, **14**, 1621-1628.

14 S. Paek, N. Cho, K. Song, M-J. Jun, J. K. Lee and J. Ko, *J. Phys. Chem. C*, 2012, **116**, 23205- 23213.

15 Y. Liu, Y. Yang, C-C. Chen, Q. Chen, L. Dou, Z. Hong, G. Li and Y. Yang, *Adv. Mater.,* 2013, **25**, 4657-4662.

16 D. Yang, Q. Yang, L. Yang, Q. Luo, Y. Huang, Z. Lu and S. Zhao, *Chem. Commun.,* 2013, **49**, 10465-10467.

17 D. Bagnis, L. Beverina, H. Huang, F. Silvestri, Y. Yao, H. Yan, G. A. Pagani, T. J. Marks and A. Facchetti, *J. Am. Chem. Soc.*, 2010, **132**, 4074-4075.

18 J. E. Johns, E. A. Muller, J. M. J. Frechet and C. B. Harris, *J. Am. Chem. Soc.*, 2010, **132**, 15720-15725.

19 C. Wu, P. I.Djurovich and M. E. Thompson, *Adv. Funct. Mater.*, 2009, **19**, 3157-3164.

20 A. W. Hains, Z. Q. Liang, M. A. Woodhouse and B. A. Gregg, *Chem. Rev.*, 2010, **110**, 6689-6735.

21 S. Wang, L. Hall, V. V. Diev, R. Haiges, G. Wei, X. Xiao, P. I. Djurovich, S. R. Forrest and M. E. Thompson, *Chem. Mater.*, 2011, **23**, 4789-4798.

22 M. Sonntag, K. Kreger, D. Hanft, P. Strohriegl, S. Setayesh and D. de Leeuw, *Chem. Mater.*, 2005, **17**, 3031-3039.

23 T. K. Chaitanya and R. Nagarajan, *Org. Biomol. Chem.*, 2011, **9**, 4662-4670.

24 D. H. R. BArton, R. K. Haynes, G. Leclerc, P. D. Magnus and I. D. Menzies, *J. Chem.*

Soc., Perkin Trans. 1, 1975, 2055-2065.

25 B. Walker, C. Kim and T. Q. Nguyen, *Chem. Mater.*, 2011, **23**, 470-482.

26 J. Pommerehne, H. Vestweber, W. Guss, R.F. Mahrt, H. Bassler, M. Porsch and J. Daub, *Adv. Mater.*, 1995, **7**, 551-554.

27 C. J. Brabec, A. Cravino, D. Meissner, N. S. Sariciftci, T. Fromherz, M. T. Rispens, L. Sanchez and J. C. Hummelen, *Adv. Funct. Mater.*, 2001, **11**, 374-380.

28 J. Dai, K. Zhou, M. Li, H. Sun, Y. Chen, S. Su, X. Pu, Y. Huang and Z. Lu, *Dalton Trans.*, 2013, **42**, 10559-10571.

29 Q. Yang, D. Yang, S. Zhao, Y. Huang, Z. Xua, X. Liu, W. Gong, X. Fan, Q. Huang and X. Xu, *Appl. Surf. Sci.*, 2013, **284**, 849-854.

30 J. Bendig, U. Schedler, T. Harder, P. Wessig, J. Lobedank and W. Grahn, *J. Photochem. Photobiol. A*, 1995, **91**, 53-57.

31 J. V. Ros-Lis, R. Martínez-Máenz, F. Sancenón, J. Soto, M. Spieles and K. Rurack, *Chem. Eur. J.*, 2008, **14**, 10101-10114.

32 A. Mishra, G. B. Behera, M. M. G. Krishna and N. Periasamy, *J. Lumin.*, 2001, **92**, 175-188.

33 H. Hoppe, M. Niggemann, C. Winder, J. Kraut, R. Hiesgen, A. Hinsch, D. Meissner and N. S. Sariciftci, *Adv. Funt. Mater.*, 2004, **14**, 1005-1011.

34 V. D. Mihailetchi, H. X. Xie, B. de Boer, L. J. A. Koster and P. W. M. Blom, *Adv. Funt. Mater.*, 2006, **16**, 699-708.

35 A. J. Heeger, *Adv. Mater.*, 2014, **26**, 10-28.

36 J. L. Brédas, D. Beljonne, V. Coropceanu and J. Cornil, *Chem. Rev.*, 2004, **104**, 4971-5003.

Graphical

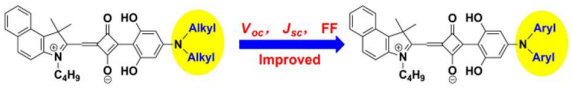

N,N-Diarylamino end-capping strategy towards asymmetrical squaraines with simultaneously enhanced V_{oc}, J_{sc} and FF in solution-processed small molecule organic solar cells.